CEAS-GNC-2024-031

EuroGNC
Bristol, UK
June 11th-13th 2024

Admittance Control Strategy for the Emulation of Space Debris Capture in a Ground Robotic Facility

Barış Can Yalçın Research Associate, Space Robotics (SpaceR) Research Group, Interdisciplinary Centre for Security, Reliability and Trust (SnT), University of Luxembourg, 6 Rue Richard Coudenhove-Kalergi, 1359 Kirchberg-Luxembourg. bariscan.yalcin@uni.lu

Mohatashem Reyaz Makhdoomi Doctoral Candidate, Space Robotics (SpaceR) Research Group, Interdisciplinary Centre for Security, Reliability and Trust (SnT), University of Luxembourg, 6 Rue Richard Coudenhove-Kalergi, 1359 Kirchberg-Luxembourg. mohatashem.makhdoomi@uni.lu

Maxime Hubert Delisle Doctoral Candidate, Space Robotics (SpaceR) Research Group, Interdisciplinary Centre for Security, Reliability and Trust (SnT), University of Luxembourg, 6 Rue Richard Coudenhove-Kalergi, 1359 Kirchberg-Luxembourg. maxime.hubertdelisle@uni.lu

Xiao Li Doctoral Candidate, Space Robotics (SpaceR) Research Group, Interdisciplinary Centre for Security, Reliability and Trust (SnT), University of Luxembourg, 6 Rue Richard Coudenhove-Kalergi, 1359 Kirchberg-Luxembourg. xiao.li@uni.lu

Miguel Olivares-Mendez Professor, Space Robotics (SpaceR) Research Group, Interdisciplinary Centre for Security, Reliability and Trust (SnT), University of Luxembourg, 6 Rue Richard Coudenhove-Kalergi, 1359 Kirchberg-Luxembourg. miguel.olivaresmendez@uni.lu

Carol Martinez Research Scientist, Space Robotics (SpaceR) Research Group, Interdisciplinary Centre for Security, Reliability and Trust (SnT), University of Luxembourg, 6 Rue Richard Coudenhove-Kalergi, 1359 Kirchberg-Luxembourg. carol.martinezluna@uni.lu

ABSTRACT

The rapid increase in space debris within Low-Earth Orbit (LEO) has prompted space agencies to consider Active Debris Removal (ADR) systems as a viable solution for ensuring the safety of space activities. While current capturing systems are primarily designed for large, cooperative satellites, there remains a significant threat from numerous uncooperative small debris in LEO. To address this challenge, we proposed a Flexible Capturing System called FlexeS that includes an Active Compliance Unit (ACU) and a Passive Compliance Unit (PCU) to dissipate impact energy and expanding the range of capturable space debris. This paper presents admittance control strategy created to emulate FlexeS' ACU with UR10e robotic arms located in the Zero-G Lab facility at UniLu. Results confirm the effectiveness of the admittance control strategy to emulate the ACU behaviour during space debris capture. The study has been conducted under the project "High fidELity tEsting eNvironment for Active Space Debris Removal - HELEN".

Keywords: Orbital Robotics; Active Space Debris Removal; Orbital Robotics Facilities; Force feedback

Nomenclature

F_i = External force
F_a = Linear actuator force
m_d = Desired mass gain for admittance controller
m_s = Mass of satellite
m_e = Second mass (ACU and PCU components)
m_c = Third mass (FlexeS' tip)
m_{deb} = Debris' mass
b_d = Desired damping gain for admittance controller
b_s = Damping coefficient of PSU
k_d = Desired spring gain for admittance controller
k_s = Spring coefficient of PSU
x_s = Position of satellite
x_a = Position of linear actuator
x_e = Position of second mass
x_c = Position of third mass
x = Measured end-effector-position of the UR10e robot
x_d = Desired position of the linear actuator of ACU
x_d^* = UR10e robot's desired end-effector position

1 Introduction

In space, the number of space debris from different sources, for instance dead or broken satellites, has been exponentially growing, generating a massive threat to all devices in Earth's orbit [1, 2]. To fight against this instability, missions focused on ADR have become crucial [3]. These missions employing various capture mechanisms categorized under the Energy-Transfer Classification (ET-Class) [4]. An ADR mission comprises several essential stages, starting from the spacecraft's launch from Earth to the moment when the chaser satellite, connected with the debris, re-enters the atmosphere. These phases include berthed standby (where the chaser satellite is aboard and linked to the hosting platform), ejection (encompassing the rocket launch until payload ejection), Far-Range Approach (reaching the hold point near the target), capturing, and post-capture (prepared for de-orbiting). The capturing phase stands out as the most critical. Given minimal collaboration between the chaser and the target (lacking communication, fiducial markers, or capture interfaces), capturing uncooperative debris poses a significant challenge. This phase is prone to mission failure and debris generation, leading to potentially dire consequences. The Capturing Phase consists of three sub-phases: Pre-Capture, Soft-Capture, and Hard-Capture. These sub-phases are responsible for approach preparation, impact absorption and stabilization, and securing the attachment of the debris. This paper specifically focuses on the Soft-Capture sub-phase. During this stage, the servicer satellite's thrusters are activated to approach the debris and make initial contact. It is essential that the first impact between the capturing mechanism and the debris is gentle to prevent the debris from being pushed away.

Due to the high demand for reliability in capturing uncooperative debris, compliant robotic systems are essential. The FlexeS, as illustrated in Fig. 1, incorporates both passive and active compliance, designed to fit within a CubeSat architecture, for capturing small, box-shaped debris in LEO. As depicted in Fig. 1, FlexeS consists of passive and active compliant units, referred to as PCU and ACU respectively. This integration aims to reduce shocks, minimize hard contacts. The PCU serves two main functions: ensuring a softer impact with the debris and adhering to the debris surface to prevent it from moving away. This unit comprises flexible legs, spherical joints, and adhesive pads. The ACU is directly connected to the PCU and integrates controllable electromechanical linear actuators, all linked to a Force/Torque (F/T) sensor at their base. Active compliance is achieved through the active control of these linear actuators along the capture axis. Admittance control is an effective strategy for ensuring the initial contact with

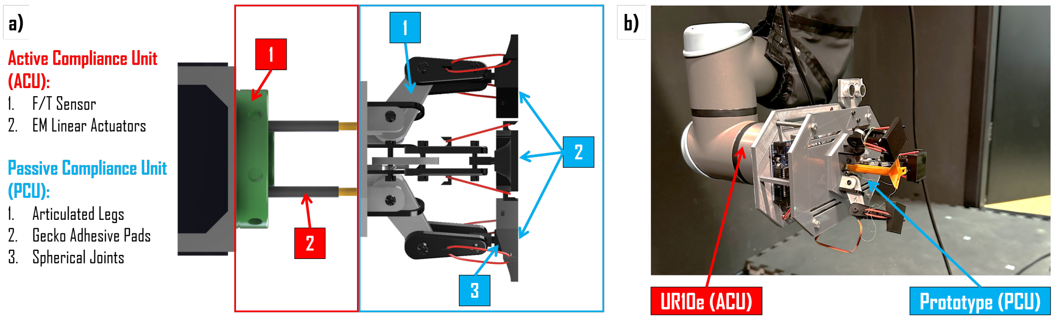

Fig. 1 The Flexible Capturing System FlexeS, a) FlexeS, b) ACU emulation and PCU prototype in the Zero-G Lab

space debris. The main reason of this need is that energy dissipation and energy storage between the chaser and target satellites must be realized in a controlled way. Otherwise, the chaser satellite's capturing mechanism may damage the target satellite, and even may generate more debris in space.

To validate the capturing mechanism, on-ground test, verification and validation of FlexeS will be conducted on the Zero-G Lab facility of the University of Luxembourg. The emulation of the capturing phase, which includes the first contact will be done using the robotic arms located on the facility. Robotic manipulators in on-ground test facilities can play various important roles as being different components of ADR systems [5–16]. In on-ground emulation, ADR systems are mostly tested as integrated to the end-effector of robotic manipulators that make them act as if they were in space [17–20]. In this paper, an UR10e robotic arm located at the Zero-G Lab will be used to emulate the behavior of the ACU (the linear actuator) of the robotic capturing mechanism presented in [21]. We present and test the admittance control strategy created for the emulation of the behaviour of the linear actuator. The latter allows to get preliminary evaluation and validation of the behaviour of the hybrid compliant system (ACU+PCU) during the capturing process.

The structure of the paper is given as follows; The Flexible Capturing System configuration is presented in Section-II. The Zero-G Lab, on-ground orbital robotics testing facility of SnT and its equipment are presented in Section III. Emulation of ACU, Admittance controller and their integration to the infrastructure of the facility are given in Section-IV. The experiment results are shown in Section V, and finally the conclusion and future studies are stated in Section-VI.

2 The Flexible Capturing System

Capturing uncooperative space debris requires high reliability to guarantee that the debris is not pushed away and to ensure sufficient contact time for the capture. To guarantee this soft capture, we proposed the concept of a hybrid-compliant system, shown in Fig. 1, that integrates an Active Compliance Unit (ACU) with tunable stiffness and a Passive Compliance Unit (PCU), with constant stiffness. Together they form the Soft Capture Unit (SCU) the capturing mechanism part of FlexeS (The Flexible Capturing System).

The schematic of the equivalent three-body of the FlexeS inside of CubeSat as interacting with a space debris is given in Fig. 2. The three-body diagram features a primary body (CubeSat) and the hybrid-compliant FlexeS for soft capture, modeled as an equivalent system with three masses: m_s, m_e and m_c. m_s represents the satellite's mass, with its position indicated by x_s. The moving part of the ACU's actuators, the plate separating the ACU and PCU, and the PCU's upper legs are combined into a second rigid body with mass m_e. The lower legs and gecko adhesive pads are combined into a third rigid body with mass m_c. The center of mass (CM) positions of m_s and m_e are denoted by x_s and x_e respectively, while the position of the mechanism's tip is represented by x_c. The debris is treated as a rigid body with mass m_{deb}, and the contact point on the debris with the mechanism's tip is denoted by x_{deb}. F_i is the impact force caused by the space debris. F_a is the force generated by the linear actuator of the ACU. The model of Fig. 2 representing ADR dyanmics (including FlexeS and CubeSat dynamics) is given with the following equations.

$$F_a = m_d \ddot{x}_s \tag{1}$$

$$F_a = m_d \ddot{x}_a \tag{2}$$

$$F_a - F_i = m_e \ddot{x}_e + m_c \ddot{x}_c + b_s(\dot{x}_e - \dot{x}_c) + k_s(x_e - x_c) \tag{3}$$

$$F_i = m_{deb} \ddot{x}_{deb} \tag{4}$$

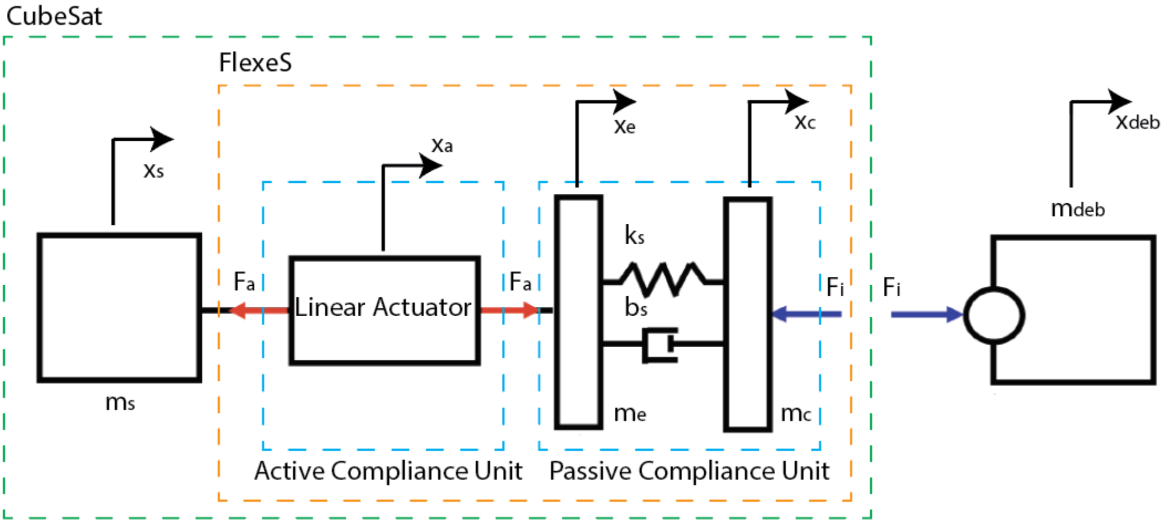

Fig. 2 Schematic of the equivalent three-body block diagram of the CubeSat-ADR system

For the emulation scenario of the FlexeS's ACU part in the Zero-G Lab, the important issues to consider are the generation of the parameters F_a and x_a on the end-effector of the UR10e robot. Depending on the control strategy we want to implement for the ACU, we will have:

- For impedance control. The input/output sequence must be $\rightarrow x_a, \rightarrow F_a$.
- For admittance control. The input/output sequence must be $\rightarrow F_a, \rightarrow x_a$.

In our previous paper [22], we conducted a simulation study of an impedance control strategy for FlexeS' ACU assuming that FlexeS' ACU actuator receives position data as input, and gives force data as output. However, because the UR10e robots do not allow sending torque commands, the validation of the impedance control strategies face implementation challenges. Therefore, for the on-ground emulation of the ACU in the Zero-G Lab, the admittance control strategy is implemented.

3 The Zero-G Lab Robotic Facility

As shown in Fig. 3, the Zero-G lab constructed at the University of Luxembourg was utilized for test the control strategies for emulation of contact dynamics. The facility has been used to emulate on-orbit

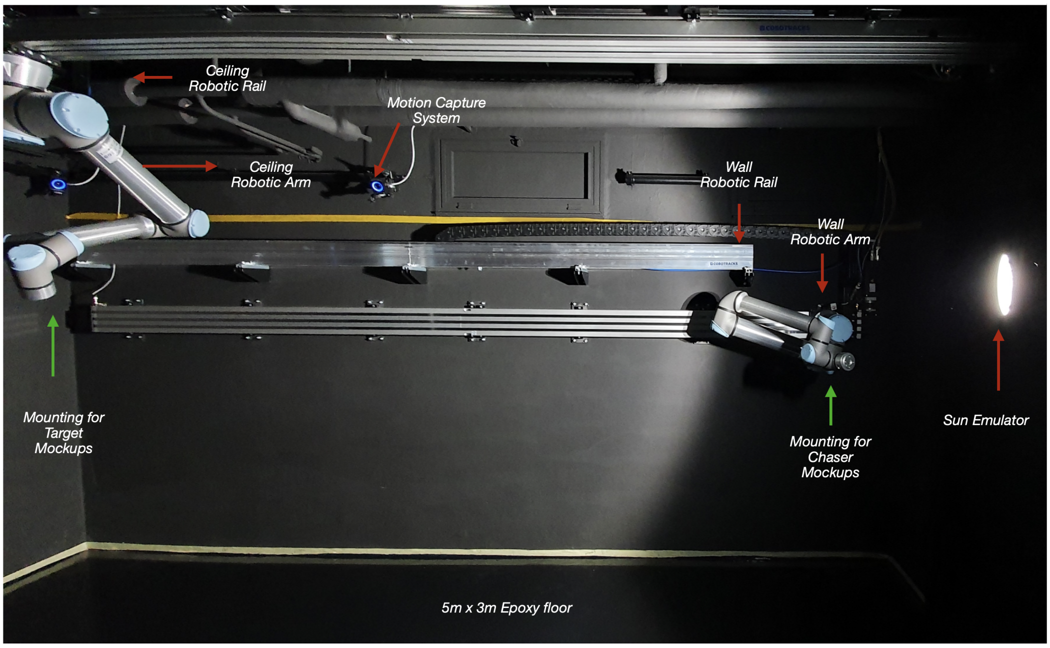

Fig. 3 **The Zero-G Lab at the SnT-UniLu**

scenarios such as rendezvous, vision-based navigation and free-floating satellite dynamics[23–25]. This facility is equipped with:

- Two UR10e robotic arms [26], mounted on motion-controlled rails.
- A super-flat epoxy floor.
- Two floating platforms powered using pneumatic systems [27].

Sensing modalities include:

- A motion capture systems (MCS) [28] in combination with different cameras to facilitate pose estimation of different objects during experimentation with sub-millimeter accuracy.
- External force torque sensors [29] with adjustable sampling frequency/noise levels (for different applications) mounted at the flange of robotic manipulators to help with experiments involving force feedback.

For communication, control and exchange of data, the above mentioned components are connected over a hardware-agnostic ROS Network facilitating the addition of any hardware system to be used during various types of experiments. Linux based dedicated computers are used each for robot control, image-processing and simulation of orbital dynamics.

A general overview of Zero-G Lab is available in the following video, named The Zero-G Lab: Testing in Micro-Gravity Environment. Detailed information about the construction and utilization of the facility is described in [6]. Within the scope of this work, the following elements of the facility were utilized during experimentation to test the control strategies for contact-dynamics emulation:

Table 1 **Hardware Utilization for Contact Dynamics Emulation**

Hardware Component	Function
Wall-mounted robotic arm	Motion Emulation of Capturing Mechanism
Externally mounted F/T sensor	Contact force and torque measurement
Floating platform	Floating Space Debris Emulation

As F/T sensors being used in orbital robotics facilities must satisfy certain hardware requirements, such as max allowed noise, sampling frequency *etc.* readings were obtained from F/T sensor at a sampling frequency of 500 Hz with 135 mN average noise [29]. There is a possibility to increase the sampling frequency for better contact emulation, or even decrease the noise in the F/T measurements. However, one is achieved at the cost of other. The sampling frequency and allowed average noise was chosen on the premise that the contact forces generated are not buried by the noise during the measurements.

4 Emulation of Active Compliant Unit for Space Debris Capture

The servicing satellite's Guidance, Navigation, and Control (GNC) system rendezvous and synchronizes its motion with the debris. Initially, the ADR system remains undeployed within the CubeSat architecture. During the soft capture phase, the servicer satellite activates its thrusters to approach the debris and make initial contact. This first contact between the capturing mechanism and the debris needs to be gentle. Therefore, we propose a hybrid-compliant system for soft capture. This system combines passive and active compliance components to minimize shocks and residual vibrations. The objective of the hard capture phase is to establish a secure link between the servicer satellite and the debris, creating a reliable bond suitable for deorbiting. Following the soft capture, the hard capture mechanism will be activated to fold and conform to the shape of the debris.

Upon contact, the flexible legs articulate naturally, providing initial damping of the impact's vibrations and preventing an elastic collision between the two entities, where both momentum and kinetic energy are conserved. The fixed stiffness of the PCU allows the legs to articulate while maintaining contact with the debris surface. During this phase, the PCU is not the only component in action; the ACU is also activated upon impact. When the Soft Compliance Unit (SCU) makes contact with the debris, the force exerted on the ADR system's tip is transmitted to the ACU's controller. Consequently, the electromechanical linear actuators respond by reducing their length, thereby providing an additional set of virtual springs and dampers based on the contact force. Thus, ACU has been emulated using UR10e robots of the Zero-G Lab.

The block diagram of the integration of the admittance control scheme applied to the UR10e robot of the Zero-G Lab can be seen in Fig. 4. The first row represents the the emulation of admittance control of the linear motor of FlexeS. In the second row, we merge the emulation with the simulation model of FlexeS. The change in the coefficients will exhibit distinct energy dissipation characteristics. Depending on the type of debris material, a specific coefficient configuration can be employed. For instance, coefficient configuration with lower damping properties can be employed for fragile or brittle debris. Regulating the energy dissipation during the soft-capture process will prevent the debris from breaking or sustaining damage, providing us with a significant advantage.

UR10e is essentially a position-controlled robot, meaning it allows control of the robot via position and velocity setpoints. It is unlike a torque-controlled robot which allows sending torque commands directly to the manipulator. This makes the UR10e robot an ideal candidate for admittance control-based strategies, as implementing impedance control requires access to the torque interface, which is not accessible for the UR10e robot. In this case, the admittance modality is implemented via an F/T sensor mounted on the flange of the position-controlled robot.

Admittance control is a control technique enabling a robot to track external forces by computing the intended position, velocity, and occasionally acceleration based on the virtual object's equation of motion, responding to external forces. Once the external force parameter is removed from the end-effector, the UR10e robots stays at the latest position.

The controller is given in Eq. 5. The controller receives the input from the F/T sensor, and generates the desired position, x_d for FlexeS. This value is fed to the Jacobian Pseudo Inverse Control block with x, which is UR10e's measured end-effector position, as the desired position (since the FlexeS' dynamics

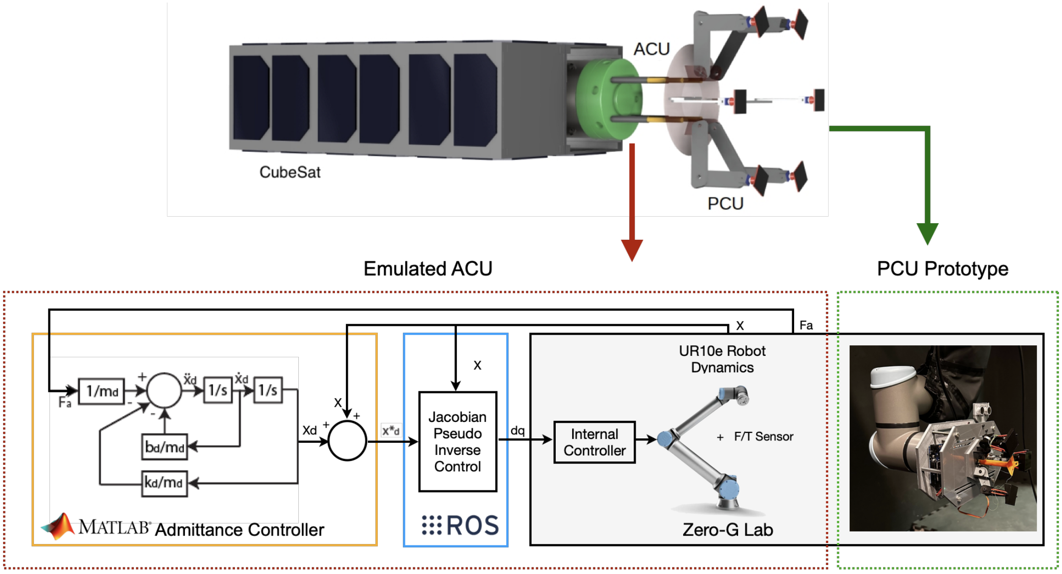

Fig. 4 The Block diagram for the emulation of active compliance unit of FlexeS

does know where the UR10e robot's end-effector in the lab), so that x_d^*, which is the desired position of the UR10e's end-effector to mimic the tip of FlexeS, is generated. The x_d^* signal is propagated to the internal controller of the UR10e robot via the Jacobian Inverse Control block as incremental joint position d_q post which the robot executes the desired motion.

$$m_d \ddot{x}_{a,d} + b_{a,d} \dot{x}_{a,d} + k_d x_{a,d} = F_a \tag{5}$$

The coefficients of the admittance controller are given in Table 2. The coefficients have been chosen to prevent collisions with the workspace of the UR10e robot and to avoid hitting the walls of the Zero-G Lab.

Table 2 Coefficients of the controllers

Coefficient	m_d	b_d	k_d
Value	1 kg	3 Ns/m	5 N/m

5 Experiment and Results

To realize this scenario in our study, a probe has been integrated to the end-effector of UR10e robot as shown in Fig. 5a. As preliminary validation of the controller frameworks, the external force, F_a, onto the probe has simply been applied by hand as shown in Fig. 5b. Future experiments, the contact tests will involve impact scenarios using floating platforms, and the probe will be replaced with FlexeS.

The experiment result is given in Fig. 6. As can be seen, once the F/T sensor located on the probe is triggered, the UR10e's end-effector starts emulating the FlexeS. The force data is fed to the admittance controller which generates the desired admittance behavior of FlexeS' ACU, and then this data is fed to UR10e robot's end-effector. The simulation and experiment outputs show similar profile, and the end-effector stays at its final position after the force input is released from the F/T sensor.

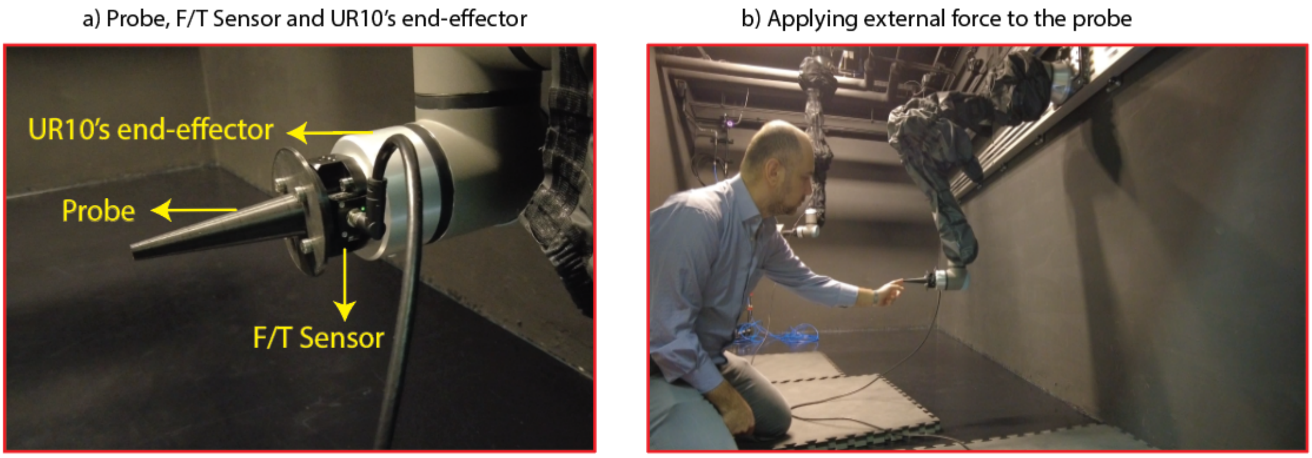
a) Probe, F/T Sensor and UR10's end-effector

b) Applying external force to the probe

Fig. 5 a) Probe, F/T sensor and UR10e robot's end-effector, b) External force on the probe

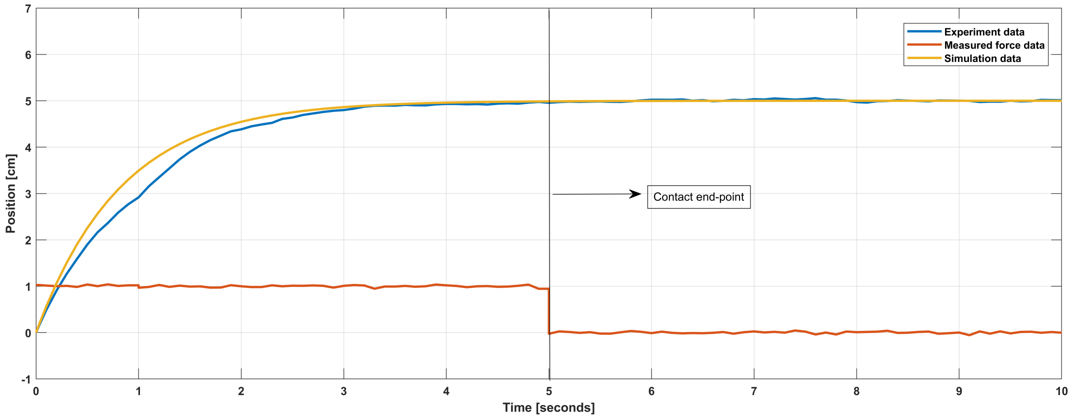

Fig. 6 The applied force and the position change of the end-effector of UR10e robot

6 Conclusion

This study has adapted model reference admittance control strategy as integrated with the internal control approach to off-the-shelf product UR10e robots located in SnT's Orbital Robotics Facility, the Zero-G Lab. The admittance controller created in MATLAB environment and communicates with ROS package of UR10e robot through ROS infrastructure of the Zero-G Lab. The experiment result shows that the admittance control strategy has successfully been implemented. Future studies will include 1- the integration of the PCU of FlexeS to the end-effector of UR10e robot. Therefore, the whole FlexeS will be emulated, 2- As free-floating object, floating platform of the Zero-G Lab will be used, 3- the admittance controller strategy will be expanded to more than single DoF, 4- the implementation challenges of impedance controller will be researched.

Acknowledgments

This study has been conducted by SpaceR under Luxembourg National Research Fund (FNR) - BRIDGES funding for "High fidELity tEsting eNvironment for Active Space Debris Removal - HELEN", project ref: BRIDGES2021/MS/15836393.

References

[1] P. Bernhard, M. Deschamps, and G. Zaccour. Large satellite constellations and space debris: Exploratory analysis of strategic management of the space commons. *European Journal of Operational Research*, 304(3):1140–1157, 2023. ISSN: 0377-2217. DOI: https://doi.org/10.1016/j.ejor.2022.04.030.

[2] J. Drmola and T. Hubik. Kessler syndrome: System dynamics model. *In:Space Policy*, pages 29–39, 2018. DOI: 10.1016/j.spacepol.2018.03.003.

[3] J. C. Liou. Active debris removal and the challenges for environment remediation. *Report - NASA Orbital Debris Program Office, NASA Johnson Space Center, Houston, Texas, USA*, 2012.

[4] B. C. Yalçın et al. Et-class: An energy transfer-based classification of space debris removal methods and missions. *Frontiers in Space Technologies*, 3:23, 2022. DOI: 10.3389/frspt.2022.792944.

[5] M. Olivares-Mendez et al. Establishing a multi-functional space operations emulation facility: Insights from the zero-g lab. *SSRN*, 2023. DOI: https://dx.doi.org/10.2139/ssrn.4602588.

[6] M. Olivares-Mendez et al. Zero-g lab: A multi-purpose facility for emulating space operations. *Journal of Space Safety Engineering*, pages 509 – 521, 2023. DOI: https://doi.org/10.1016/j.jsse.2023.09.003.

[7] J. Artigas et al. The oos-sim: An on-ground simulation facility for on-orbit servicing robotic operations. In *2015 IEEE International Conference on Robotics and Automation (ICRA)*, pages 2854–2860. IEEE, 2015. DOI: https://doi.org/10.1109/ICRA.2015.7139588.

[8] H. Benninghoff et al. European proximity operations simulator 2.0 (epos)-a robotic-based rendezvous and docking simulator. *Journal of large-scale research facilities (JLSRF)*, 2017. DOI: 10.17815/jlsrf-3-155.

[9] L. Cassinis et al. On-ground validation of a cnn-based monocular pose estimation system for uncooperative spacecraft. In *8th European Conference on Space Debris, Darmstadt, Germany*, 2021. DOI: https://doi.org/10.1016/j.actaastro.2022.04.002.

[10] H. Krüger and S. Theil. TRON-hardware-in-the-loop test facility for lunar descent and landing optical navigation. *IFAC Proceedings Volumes*, 43(15):265–270, 2010.

[11] H. Kolvenbach and K. Wormnes. Recent developments on orbit, a 3-dof free floating contact dynamics testbed. In *13th International Symposium on Artificial Intelligence, Robotics and Automation in Space (i-SAIRAS 2016)*, volume 6, 2016.

[12] P. Tsiotras. Astros: A 5dof experimental facility for research in space proximity operations. In *AAS Guidance and Control Conference*, volume 114, 2014.

[13] M. Wilde et al. Orion: A simulation environment for spacecraft formation flight, capture, and orbital robotics. In *2016 IEEE Aerospace Conference*, pages 1–14. IEEE, 2016. DOI: 10.1109/AERO.2016.7500575.

[14] X. Li et al. Exploring nvidia omniverse for future space resources missions. *ESRIC Space Resources Week, Luxembourg*, 2022.

[15] X. Li et al. Emulating active space debris removal scenarios in zero-g lab. *SnT Assessment Day, Luxembourg*, 2022.

[16] K. Aggarwal et al. Enabling elements of simulations digital twins and its applicability for information superiority in defence domain. *NATO Modelling and Simulation Group (NMSG) Symposium 2022 STO-MP-MSG-197*, 2022.

[17] Vladimir Aslanov and Alexander Ledkov. 2 - space debris problem. https://www.sciencedirect.com/science/article/pii/B9780323992992000045, 2023. ISBN: 978-0-323-99299-2. DOI: https://doi.org/10.1016/B978-0-323-99299-2.00004-5.

[18] C. Bonnal. Active debris removal recent progress and current trends. *Acta Astronautica*, pages 51–60, 2013. DOI: https://doi.org/10.1016/j.actaastro.2012.11.009.

[19] G. Borelli, G. Gaias, and C. Colombo. Rendezvous and proximity operations design of an active debris removal service to a large constellation fleet. *Acta Astronautica*, 205:33–46, 2023. ISSN: 0094-5765. DOI: https://doi.org/10.1016/j.actaastro.2023.01.021.

[20] R.M. Færgestad et al. Coupled finite element-discrete element method (fem/dem) for modelling hypervelocity impacts. *Acta Astronautica*, 203:296–307, 2023. ISSN: 0094-5765. DOI: https://doi.org/10.1016/j.actaastro.2022.11.026.

[21] M. Hubert Delisle et al. Hybrid-compliant system for soft capture of uncooperative space debris. *Applied Sciences*, 13(13), 2023. ISSN: 2076-3417. DOI: 10.3390/app13137968.

[22] O. O. Christidi-Loumpasefski et al. Adaptive control scheme for space debris capture in the presence of mass and inertia uncertainty. *IEEE Access*, pages 38304–38314, 2024. DOI: 10.1109/ACCESS.2024.3374109.

[23] Vivek Muralidharan, Mohatashem Reyaz Makhdoomi, Augustinas Žinys, Bronislovas Razgus, Marius Klimavičius, Miguel Olivares-Mendez, and Carol Martinez. On-ground validation of orbital gnc: visual navigation assessment in robotic testbed facility. *Astrodynamics*, pages 1–25, 2024.

[24] Vivek Muralidharan, Mohatashem Reyaz Makhdoomi, Kuldeep Rambhai Barad, Lina María Amaya-Mejía, Kathleen C Howell, Carol Martinez, and Miguel Olivares-Mendez. Rendezvous in cislunar halo orbits: Hardware-in-the-loop simulation with coupled orbit and attitude dynamics. *Acta Astronautica*, 211:556–573, 2023.

[25] Mohatashem Reyaz Makhdoomi, Vivek Muralidharan, Kuldeep R Barad, Juan Sandoval, Miguel Olivares-Mendez, and Carol Martinez. Emulating on-orbit interactions using forward dynamics based cartesian motion. *arXiv preprint arXiv:2209.15406*, 2022.

[26] Universal robots. `https://www.universal-robots.com/products/ur10-robot/`. Accessed: 2024-05-31.

[27] B. C. Yalçın et al. Lightweight floating platform for ground-based emulation of on-orbit scenarios. *IEEE Access*, pages 94575 – 94588, 2023. DOI: https://doi.org/10.1109/ACCESS.2023.3311202.

[28] Optitrack motion capture system. `https://optitrack.com/`. Accessed: 2024-05-31.

[29] Sensone 6-axis force torque sensor. `https://www.botasys.com/force-torque-sensors/sensone`. Accessed: 2024-05-31.